J. Fluid Mech. (2005), *vol.* 533, *pp.* 269–296.
doi:10.1017/S0022112005004209 Printed in the United Kingdom

Flow past a cylinder close to a free surface

By P. REICHL, K. HOURIGAN AND M. C. THOMPSON

Fluids Laboratory for Aeronautical and Industrial Research (FLAIR), Department of Mechanical Engineering, PO Box 31, Monash University, Melbourne, Victoria 3800, Australia

(Received 26 July 2004 and in revised form 25 January 2005)

Two-dimensional flow past a cylinder close to a free surface at a Reynolds number of 180 is numerically investigated. The wake behaviour for Froude numbers between 0.0 and 0.7 and for gap ratios between 0.1 and 5.0 is examined. For low Froude numbers, where the surface deformation is minimal, the simulations reveal that this problem shares many features in common with flow past a cylinder close to a no-slip wall. This suggests that the flow is largely governed by geometrical constraints in the low-Froude-number limit.

At Froude numbers in excess of 0.3–0.4, surface deformation becomes substantial. This can be traced to increases in the local Froude number to unity or higher in the gap between the cylinder and the surface. In turn, this is associated with supercritical to subcritical transitions in the near wake resulting in localized free-surface sharpening and wave breaking. Since surface vorticity is directly related to surface curvature, such high surface deformation results in significant surface vorticity, which can diffuse and then convect into the main flow, altering the development of Strouhal vortices from the top shear layer, affecting wake skewness and suppressing the absolute instability. The variations of parameters such as Strouhal number and formation length are provided for Froude numbers spanning the critical range.

At larger Froude numbers, good agreement is obtained with recently published experimental investigations. The previously seen metastable wake states are observed to occur for similar system parameters to the experiments despite the difference in Reynolds numbers by a factor of about 40. The wake state switching appears to be controlled by a feedback loop. Important elements of the feedback loop include the cyclic generation and suppression of the absolute instability of the wake, and the role of surface vorticity and vortices formed from the bottom shear layer in controlling vortex formation from the top shear layer. The proposed mechanism is presented. Shedding ceases at very small gap ratios (~ 0.1–0.2). This behaviour can be explained in terms of the fluid flux through the gap, vorticity diffusion into the surface and opposite-signed surface vorticity from the strong surface deformation.

1. Introduction

Flow past a cylinder close to a free surface has potential relevance to a large number of practical applications such as pipelines, offshore structures, submarines and power generation equipment using tidal power. While some attention has been focused on some parameter ranges, it has not yet been studied in detail. This contrasts with the related but simpler problem of flow past a cylinder in an infinite medium, which has been explored in depth over virtually all parameter ranges; for example, see review articles by Morkovin (1964), Berger & Wille (1972) and Williamson (1996). Thus, perhaps a useful viewpoint is that the influence of the free-surface can be considered

to cause changes from the infinite-medium reference case, although these deviations can, of course, be very large. In addition to the Reynolds number, $Re = \rho u d/\mu$, where u is the upstream velocity, d is the cylinder diameter, ρ is the density and μ is the molecular viscosity, the introduction of the free surface introduces two new parameters: the Froude number $Fr = u/\sqrt{gd}$, where g is the acceleration due to gravity; and the gap ratio h/d, with h the distance between the top of the cylinder and the position of the undisturbed surface.

The stability of the flow past a half-submerged cylinder as a function of Froude number has been examined by Triantafyllou & Dimas (1989). They found the wake was convectively unstable at all points downstream. Two convective instability modes can occur, with the first effectively corresponding to a symmetrical set of vortices dominant at lower Froude numbers, and the second asymptotically corresponding to a staggered array of vortices at Froude numbers greater than 1.77. Dimas & Triantafyllou (1994) later extended their investigations to examine the nonlinear interaction of a long-wavelength inviscid shear layer interacting with a free surface, potentially relevant to the current study. At low Froude numbers, the first branch of the dispersion relation leads to the development of strong oval-shaped vortices immediately beneath the free surface. In addition, sharp horizontal shear was observed near the free surface resulting in small sharp surface waves. The second branch corresponds to a free-surface elevation, which takes the form of a propagating wave. Large vortices form at higher Froude numbers and lead to high vertical shear. The two modes correspond to different forms of wave breaking with the characteristics of the first mode being large horizontal and small vertical velocities and vice versa for the second mode.

The related problem of flow past a cylinder near a no-slip surface also provides a useful point of reference for the current study. Taneda (1965) examined that flow for $0.10 \leqslant h/d \leqslant 0.60$ at $Re = 170$. At the larger gap ratio, regular vortex shedding occurred, however, at the smallest gap ratio, a single layer of vortices resulted, which became unstable after a few wavelengths downstream. For the same flow, Roshko, Steinolfson & Chattoorgoon (1975) examined the behaviour of the lift and drag forces with gap ratio. On reducing the gap ratio, the drag first increased before rapidly decreasing. This result was confirmed by Göktun (1975) who found the maximum drag occurred at $h/d \simeq 0.5$. The lift, on the other hand, monotonically increased as the cylinder approached the wall. Taniguchi & Miyakoshi (1990) extended this work to include the effect of wall boundary-layer thickness, which they found had a substantial influence at smaller gap ratios. Bearman & Zdravkovich (1978) investigated the frequency response for a cylinder near a no-slip boundary. They found that the Strouhal number drops quite rapidly as the cylinder approaches the wall, with a marked change in behaviour near a gap ratio of $h/d \simeq 0.25$. Göktun (1975) observed an initial increase in Strouhal number as the gap ratio was decreased to 0.5, with a decrease at smaller gap ratios. Similarly, Angrilli, Bergamschi & Cossalter (1982) determined the Strouhal number variation, but at much lower Reynolds numbers ($Re = 2860$ and 7640). They found the same behaviour and the same critical gap ratio as found by Göktun. Lei *et al.* (1998) considered this problem numerically for a two-dimensional cylinder at $Re = 1000$. They found weakening of shedding for $h/d = 0.30$, and suggested that the Strouhal number reaches a minimum not a maximum at $h/d = 0.50$. However, it seems likely that two-dimensional modelling is not appropriate at such Reynolds numbers, as it leads to exceptionally strong compact vortices and a very short formation length, in contrast to the real three-dimensional flow. Lei, Cheng & Kavanagh (1999) also tackled the problem experimentally. They noted the strong influence of the

boundary-layer development on the lift acting on the cylinder. Price *et al.* (2000) also considered this flow experimentally at $Re = 1200$. They found a large variation in Strouhal number and the presence of additional frequency components in the wake at smaller gap ratios as the wake became less periodic.

Also relevant to the current study is the behaviour of vortical flows near a (deformable) free surface. Yu & Tryggvason (1990) investigated the free-surface signature of unsteady two-dimensional vortex flows numerically. Their major finding was that the dominant parameter governing surface deformation is the Froude number. At small Froude numbers, the vortices interact with the free surface as though it is a rigid wall, whereas at large Froude numbers, the vortices cause significant surface deformation. Ohring & Lugt (1991) and Lugt & Ohring (1992) investigated the interaction of a two-dimensional vortex pair with a free surface, including the effects of viscosity and surface tension. For intermediate Froude numbers and low Reynolds numbers, these authors indicate that the vortices rebound from the free surface, with the degree of rebounding diminishing with increasing Reynolds number. The inclusion of viscosity gives a clearer picture of the surface interaction, with significant levels of vorticity diffusing from regions of high curvature. The presence of this secondary vorticity has a profound effect on the evolution of the primary vortices through shedding of the secondary vorticity from the surface and subsequent entrainment, resulting in considerable weakening of the primary vortices. Surface tension acts to limit strong surface curvature, thereby reducing the production of secondary vorticity at the surface (Tryggvason *et al.* 1991). This can significantly modify the interaction of vortices with a free surface at high Froude numbers if the surface tension is significant. Similarly, surface contamination can have a strong effect. Moderate surface contamination can make the surface effectively act somewhere between a no-slip and free-slip boundary (Wang & Leighton 1991; Sarpkaya 1996). Even worse, surface motion can often produce an uneven distribution of contaminants (Tryggvason 1988), thereby effectively producing a temporally and spatially varying surface boundary condition. A detailed discussion of the vorticity and free surfaces, including many illuminating examples, is given by Rood (1995). Also of interest, Lundgren & Koumoutsakos (1999) provide an interpretation enabling vorticity conservation in flows with free surfaces by allowing vorticity to be stored in surface vortex sheets.

Flow past a cylinder near a free surface was considered by Miyata, Shikazono & Kani (1990) with an experimental and numerical investigation conducted at $Re \simeq 50\,000$ and $Fr = 0.24$. They noted a sharp reduction in drag and a sharp increase in Strouhal number as the gap ratio was reduced from 0.35. They also noted the considerable weakening of shedding and introduction of other frequency components, at smaller gap ratios. They found that the drag was almost bimodal with one value for large gap ratios dropping suddenly to a smaller value at small gap ratios. This is in contradiction to the observations of Göktun (1975) and Roshko *et al.* (1975) for flow past a cylinder near a no-slip wall, who both found relatively smooth (but different) variations with gap ratio.

The flow behaviour of a cylinder near a free-surface for $Fr = 0.60$ and $h/d = 0.45$ has been considered by Sheridan, Lin & Rockwell (1995). For this parameter set, two admissible wake states were observed. Each state was found to possess limited stability such that transformations from one state to the other occurred in a time-dependent manner. Thus, the flow was catagorized as *metastable*. The fluid passing over the cylinder remained attached to the free surface when the flow was in one of the states, and it was separated in the other state. The switching could occur spontaneously

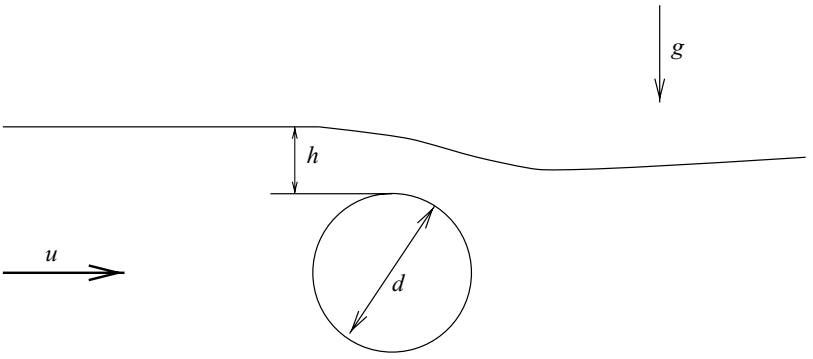

FIGURE 1. The problem set-up, and some of the important parameters.

with a very low non-dimensional frequency of the order of 10^{-3}, or be induced by artificially piercing the surface.

A region of parameter space was investigated by Sheridan, Lin & Rockwell (1997), with a wide variety of different wake behaviours noted. The jet of fluid passing over the cylinder was observed to exhibit a number of possible states including: attachment to the free surface; attachment to the cylinder; and an intermediate state in between. The previously observed metastable behaviour was also observed at gap ratios and Froude number combinations other than the pair reported in Sheridan *et al.* (1995). Both of these papers concentrate on mapping out the different wake states without providing much information on physical parameters such as shedding frequency, forces and other physical characteristics. Hoyt & Sellin (2000) confirm some of the findings of Sheridan *et al.* (1997) and provide some further details on the time-dependence. A major finding is that Kármán vortex shedding occurs at some gap ratios and that the flow field varies in a time-dependent manner.

The problem was also investigated by Warburton & Karniadakis (1997) at $Re = 100$ using a two-dimensional numerical model. They suggest that the flow features observed by Sheridan *et al.* (1997) are largely two-dimensional in nature. They provide limited information on the time-dependent forces acting on the cylinder. Reichl, Hourigan & Thompson (2003) have presented some results from computations of the flow at $Re = 180$, mainly focusing on the evolution of the vorticity field for the metastable state first described by Sheridan *et al.* (1995).

The layout of this paper is as follows. Initially, a brief description of the numerical method is presented together with supporting validation and resolution studies. After this, results from numerical simulations are given, beginning with an overview demonstrating the main effects of gap ratio and Froude number, followed by more details of the variation of physical parameters and some physical interpretations. Finally, some special cases matching previous experimental studies are explored and interpreted, including a discussion of mechanisms controlling the wake dynamics.

2. Flow modelling

2.1. *Problem set-up and important parameters*

The problem set-up is shown in figure 1, together with the important dimensions. The flow is from left to right with the cylinder submerged a distance h below the surface (under no flow conditions). The diameter of the cylinder is d and the upstream velocity is u. Since we have a free surface, the acceleration due to gravity, g, exerts

an influence and must be considered. The important physical parameters were given in § 1 and are the Reynolds number, *Re*, the Froude number, *Fr*, and the gap ratio, h/d. In the limit, $Fr \to 0$, the surface becomes a non-deformable horizontal free-slip surface. The Strouhal number, $St = fu/d$, where f is the vortex-shedding frequency in the wake is another important physical parameter characterizing the flow state.

2.2. *Numerical method*

The simulations were carried out using the computational fluid dynamics software package FLUENT. Only a brief description of points of direct relevance to the computations will be provided here, further details of the implementation can be found in the FLUENT manuals. Versteeg & Malalasekera (1995) provide an excellent description of the finite-volume method on which the package is based, while a description of the volume-of-fluid (VOF) method used to treat two-phase flows is given in Hirt & Nichols (1981).

The main computational difficulty is the deformable free-surface. There are various ways to treat this situation numerically. A potential constraint in this case is that the surface may form breaking waves at high Froude numbers, which means that computational methods that track the surface directly as a computational boundary may have difficulties. It was decided to tackle the problem using the volume-of-fluid approach. Here, both the fluid phase and the much lighter gas phase above it are treated explicitly by introducing a (fluid) volume fraction, α_1, and gas volume fraction, α_2. The combined volume fraction of both phases must satisfy the conservation property, $\alpha_1 + \alpha_2 = 1$. A conservation equation is solved to transport the volume fraction of one of the phases. The viscosity and density at any point are obtained by volume phase averaging. A single momentum equation is solved for the whole domain resulting in a shared velocity field for both phases. The surface is defined to be the locus of points where $\alpha_1 = 0.5$. In practice, the surface is represented by piecewise linear segments across each cell.

The spatial discretization chosen was the QUICK (quadratic upstream interpolation for convective kinematics) method of Leonard (1979). This is a hybrid of second-order upwinding and central-differencing for the convective terms together with central-differencing for the viscous terms. Hence, it is second-order accurate overall, although the truncation error coefficient is formally smaller than either of the constituent schemes. The temporal discretization is only first-order accurate when the VOF method is employed.

2.3. *Validation and resolution tests*

Several benchmark tests were employed to ensure that the method behaved as predicted theoretically. Poiseuille flow was modelled for a series of grids with different spatial resolutions. By comparing with the exact solution, it was possible to establish the order of the QUICK method for this case as 2.55, which is better than the theoretical prediction. The transient state of impulsively started Couette flow was used to establish the temporal accuracy as first-order, as predicted.

Benchmark deformable surface flows are more difficult to find. Two cases were examined. The first was the idealized case of fluid in a spinning bowl in a vacuum. The free surface forms a parabolic profile in the radial direction. An analytic expression for the shape is easily derived. Equilibrium solutions were computed for a series of different density and viscosity ratios. In reality, at standard conditions, the density ratio is $\rho_{water}/\rho_{air} = 811$, and the viscosity ratio is $\mu_{water}/\mu_{air} = 60$. Generally, as these ratios are increased, the real conditions of the water–air free surface are reproduced. On the other hand, the equations become stiffer, resulting in convergence problems or

at least many more iterations between time steps, as these ratios are increased. Hence, in practice, it is necessary to compromise. It was found that using $\rho_{water}/\rho_{air} = \mu_{water}/\mu_{air} = 100$, gave a solution with a relative fractional L_2 norm error of 0.00043. This was only slightly larger than the error using the accepted water/air ratios, which required considerably increased computer time. For the former case, the solution was graphically indistinguishable from the idealized solution over the entire radius except for a few points near the outer radius. It was decided that realistic solutions to free-surface (or fluid–air interface) problems could be obtained with $\rho_{fluid}/\rho_{air} = \mu_{fluid}/\mu_{air} = 100$, and these combinations were subsequently used for all further simulations.

The breaking dam problem of Martin & Moyce (1952) was used to investigate the ability of the software to model a rapidly changing surface. These authors experimentally determined the height and surge front location of an initially rectangular cross-sectioned volume of water after one of the supporting walls was destroyed impulsively at time zero. The predicted water height and surge front location both agreed, to within experimental error, over the entire time over which data were experimentally recorded.

A validation study close to the problem under consideration was flow past a fully submerged cylinder, i.e. a cylinder far removed from the free surface. Of course, this one of the most studied experimental and computational flows and accurate values of many physical parameters are available. Figure 2 shows a typical computational mesh used for simulations. This particular mesh has approximately 56 000 node points with considerable mesh concentration both around the cylinder and in the wake. For a Reynolds number of 190, this mesh gave a Strouhal number of $St = 0.191$. This is within 2 % of the accepted value of 0.194–0.195 (Williamson 1989; Barkley & Henderson 1996). The errors in the drag coefficient, C_D, the root mean square (r.m.s.) lift coefficient, C_L', and the base pressure coefficient, C_{pb}, are 1 %, 6 % and 4 %, respectively. For this mesh, the distances to the upstream, side and outflow boundaries were $L_1 = 10d$, $L_2 = 30d$ and $L_3 = 30d$, respectively. Simulations using meshes of increased dimensions led to only small changes in these physical parameters, hence it was decided that these dimensions were adequate for the purpose of exploring a large part of the parameter space with good accuracy. This domain size is broadly consistent with the domain used by Henderson (1997) for his benchmark study.

To ensure that this mesh was fine enough to resolve the flow properly for the actual flow problem considered in this paper, a resolution study was undertaken. Physical parameters were determined for $Re = 180$, $h/d = 0.40$ and $Fr = 0.20$, for this mesh and a geometrically similar finer mesh with 89 000 node points. Using Richardson extrapolation allowed the errors in the Strouhal number, drag and r.m.s. lift coefficients to be estimated as 0.3 %, 0.3 % and 7 %, respectively.

Finally, the error induced by the first-order temporal scheme was examined. For $Re = 180$, $h/d = 0.40$ and $Fr = 0.30$, the physical parameters were again determined for time steps of $\Delta t = 0.0250$ and 0.0125. For the Strouhal number and drag coefficient, the predictions varied by less than 3 %, while for the r.m.s. lift, the difference was about 5 %. To limit the amount of computer time per simulation, because of the large number of simulations required, $\Delta t = 0.025$ was chosen as an appropriate compromise.

The findings of these preliminary studies can be summarized as follows. The mesh of 56 000 node points with increased resolution near the cylinder and in the wake is sufficient to predict the Strouhal number and drag to within 5 %. The predictions of the r.m.s. drag appear to be more sensitive to both time and space resolution and the error may be larger and perhaps up to 10 %. This accuracy is believed to be acceptable for the current study. In particular, we expect the physical behaviour

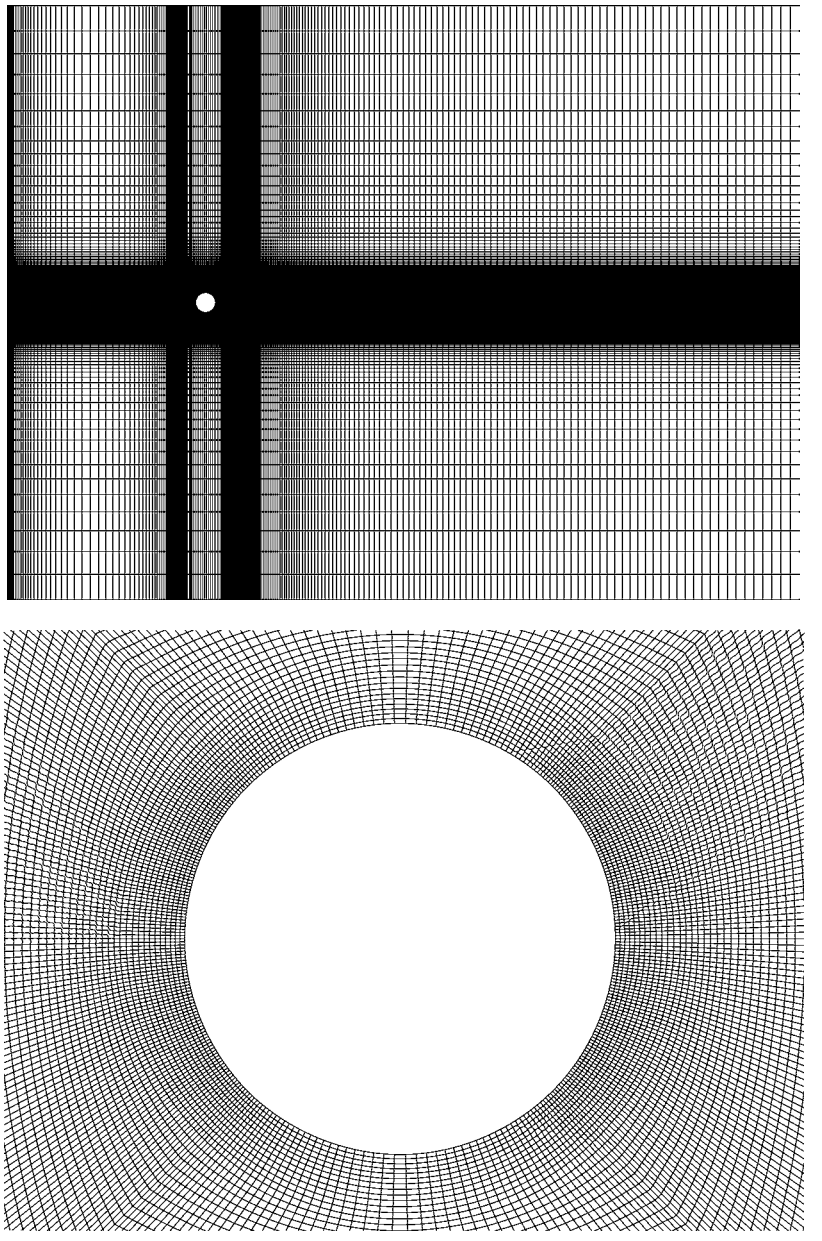

FIGURE 2. Grid used for the majority of the simulations. It contains approximately 56 000 cells.

of the wake should be captured well. Further validation and demonstrations of the correctness of this premise come from the comparison with experimental predictions provided later in this paper.

2.4. *Selection of the Reynolds number*

Sheridan *et al.* (1995) suggest that, in general, the surface behaviour and wake are quasi-two-dimensional even at the Reynolds number of their experimental studies ($Re \simeq 6000$–9000), where the flow must be fully turbulent. While it may be possible

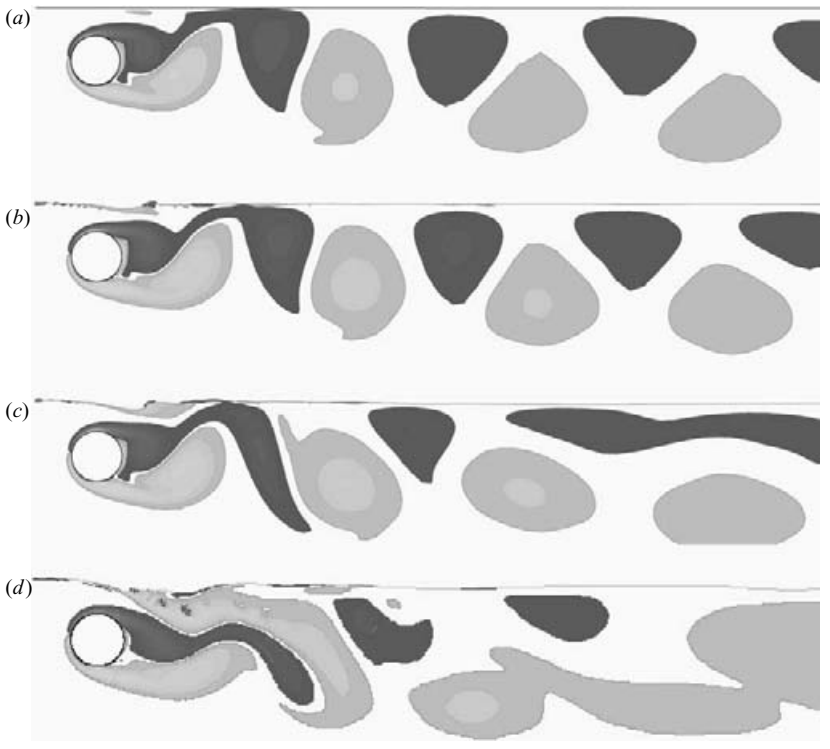

FIGURE 3. Vortex streets for a gap ratio of $h/d = 0.55$ and for Froude numbers of (*a*) $Fr = 0$, (*b*) 0.3, (*c*) 0.4 and (*d*) 0.6. Positive vorticity is shown as light grey and negative vorticity as dark grey.

to perform fully three-dimensional large-eddy simulations at such Reynolds numbers, these would be extravagantly expensive and would certainly prohibit a parameter space study, which is a key aim of this work. Because of the observed predominant two-dimensional nature of the observations, we envisaged that low-Reynolds-number two-dimensional simulations would be adequate to reproduce the main physical behaviour, and would allow the effect of various parameters to be determined. The Reynolds number chosen for the bulk of the simulations was $Re = 180$. This is close to the Reynolds number for transition to three-dimensional flow of $Re = 190$ (Barkley & Henderson 1996). While it is possible to use higher Reynolds numbers, the predictions are likely to be less relevant to the higher-Reynolds-number experiments. This is because the formation length rapidly becomes unphysically short, and the Strouhal number diverges from its near-Reynolds-number independent value of about 0.2. In addition, since the flow is almost certainly two-dimensional at $Re = 180$, the set of predictions will be a true representation of reality at $Re = 180$, and thus stand in their own right.

3. Results

3.1. *Overview of the different regimes*

Figures 3 and 4 show typical vorticity fields covering a range of Froude numbers and gap ratios. These plots provide a broad overview of the different types of wake behaviours that can occur. Figure 3 corresponds to a gap ratio of $h/d = 0.55$ and shows

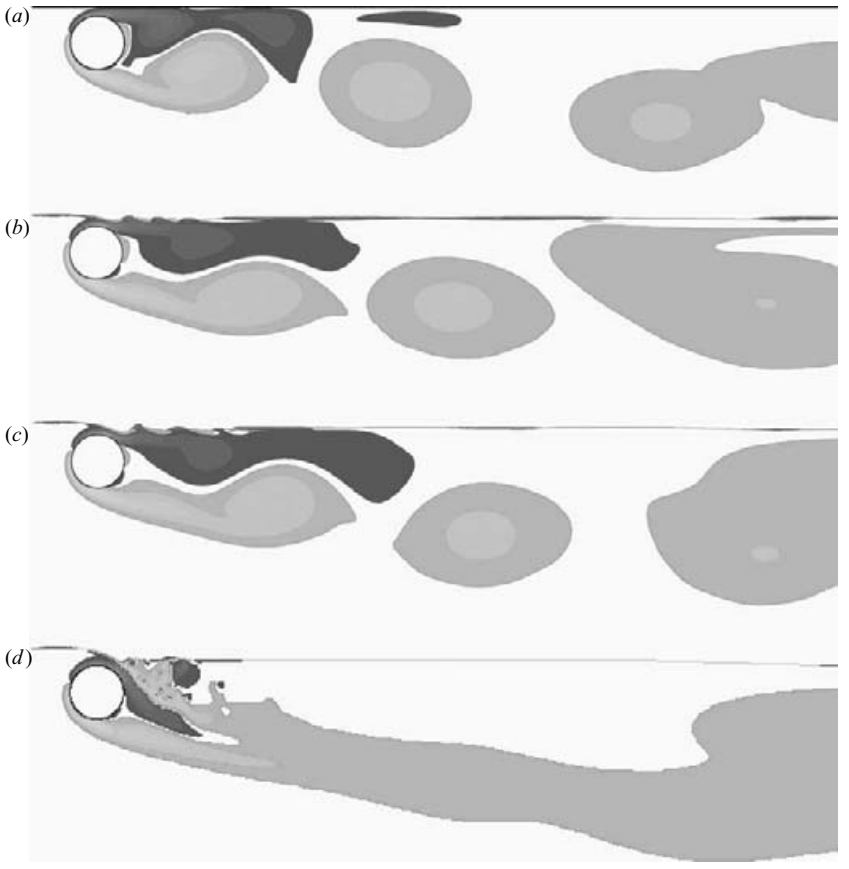

FIGURE 4. Vortex streets for a gap ratio of $h/d = 0.16$ and for Froude numbers of (*a*) $Fr = 0$, (*b*) 0.3, (*c*) 0.4 and (*d*) 0.6.

the changes in the vorticity field and free-surface behaviour as the Froude number is increased. Figure 3(*a*) provides a reference case of $Fr = 0$, a horizontal free-slip boundary. The wake is not too dissimilar to that from the reference case of flow past a cylinder submerged in an infinite medium. The wake has reasonable symmetry about the centreline, although there is some diffusion of vorticity into the surface and the centreline of the wake is directed downwards slightly. The $Fr = 0.30$ case is similar to this, except that there is some local surface distortion up to one diameter downstream of the cylinder owing to the presence of strong compact vortex structures formed from the shear layers rolling up. This ratio of the inertial to gravitational force is proportional to Fr^2, so for this case the ratio is about 10 %. This Froude number approximately marks the boundary between the low- and high-Froude-number cases. At the next highest Froude number shown, $Fr = 0.40$, there is a marked difference in the downstream wake. Here, the surface distortion is considerably larger, and the induced surface curvature leads to a diffusive flux of vorticity from the surface of opposite sign to the vorticity immediately below. This secondary vorticity is diffused outward and then convected away from the surface to cross-annihilate with the wake vorticity, causing the wake to become much more asymmetric downstream. The last case shown is for $Fr = 0.60$. Here, the wake is considerably different from the previous cases. Surface distortion is substantial, with the large amount of surface vorticity

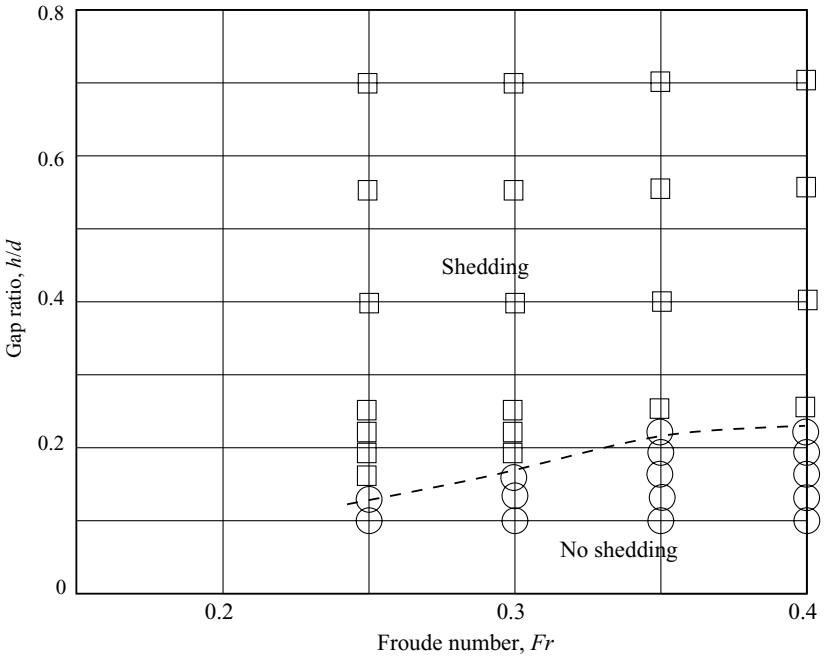

FIGURE 5. Existence or non-existence of shedding as a function of Froude number and gap ratio.

diffused and convected into the wake to interact strongly. The wake is now very much lop-sided or skewed, and much less regular.

Figure 4 shows vorticity plots for the same set of Froude numbers, but for a gap ratio of 0.16. The wake structure is quite different from the larger gap ratio cases. The formation length is significantly longer, increasing progressively as the Froude number increases. The negative (clockwise) vorticity from the top half of the wake has been largely dissipated by approximately $5d$ downstream, even in the zero Froude number case. This is due to restriction of flow in the gap and some diffusion into the surface. Thus, further downstream the wake consists of only positive (anticlockwise) Strouhal vortices originating from the bottom half of the wake. The difference between the $Fr = 0$ and $Fr = 0.3$ vorticity patterns is larger than for $h/d = 0.55$ shown in the previous figure. This is probably because the local Froude number in the vicinity of the cylinder is higher in the former case; indeed this will be explored later. At $Fr = 0.6$, the surface interaction and associated flux of surface vorticity is so large that even in the near wake shedding is suppressed. From approximately 2 diameters downstream, the wake consists of only positive vorticity. The formation length is extremely long.

3.2. *Suppression of vortex shedding*

Figure 5 shows the occurrence or non-occurrence of vortex shedding as a function of Froude number and gap ratio. Triantafyllou & Dimas (1989) showed that in the extreme case where the cylinder is only half submerged, the wake instability changes from absolute to convectively unstable. This is consistent with suppression of vortex shedding when the cylinder is placed in close proximity to the surface. We have examined Froude numbers in the range $0.25 \leqslant Fr \leqslant 0.40$, for a wide range of gap ratios. This covers the range where the Froude number starts to have a strong effect on the wake dynamics and surface distortion. For a free-slip surface ($Fr = 0$), if the

gap ratio is reduced to zero, there is no flow over the top of the cylinder and hence the wake will be one-sided. On the other hand, even for small gap ratios at low Froude numbers, there is considerable flow over the cylinder and hence considerable vorticity generated, nominally with shedding into the wake. However, the proximity to the surface causes this vorticity to diffuse into the surface, thereby leading to rapid reduction of vorticity to form vortices from the top half of the wake. As the Froude number is increased into the region where surface distortion begins to become significant ($Fr \simeq 0.3$), a flux of positive vorticity from the surface results, owing to the surface curvature induced by the nearby negative vorticity from the top half of the wake. This cross-annihilates with the wake vorticity, decreasing the wake vorticity still further. Hence, at higher Froude numbers, vortex shedding will be suppressed at larger gap ratios, as figure 5 shows.

Strictly speaking, there is some irregular vortex shedding for the higher-Froude-number small-gap-ratio cases. For instance, for $h/d = 0.19$ and $Fr = 0.40$, several frequencies were apparent in the Fourier spectrum of the cylinder lift coefficient, but the amplitudes were small and spread over broad frequency bands. In contrast, the spectrum for $h/d = 0.19$ and $Fr = 0.25$ showed a narrow band response; indeed the signal was almost sinusoidal and periodic. Price *et al.* (2000) found a number of distinct frequencies unrelated to the Kármán shedding frequency for flow past a cylinder close to a no-slip surface. They suggested that there was a frequency scaling with the separation of the wall boundary layer from the surface in addition to the dominant Kármán frequency. Two other frequencies were also apparent, being due to the addition of these frequencies and the first harmonic of the Kármán frequency. The presence of multiple frequency components appears to be similar here, despite the distinctly different surface boundary condition.

3.3. *Surface sharpening and wave breaking*

As mentioned before, surface distortion starts to have a major impact for $Fr \gtrsim 0.30$. Figure 6 focuses on the relatively sudden onset of severe surface distortion as the Froude number is incrementally increased. Figures 6(*a*) and 6(*b*) show the surface shape at times of maximum and minimum lift for gap ratios of 0.55 and 0.40, respectively, for $Fr = 0.35$. Figures 6(*c*) and 6(*d*) show the surface shape for the same gap ratios, but for $Fr = 0.40$. Clearly, the surface distortion increases substantially at the slightly higher Froude number. In fact, the surface profiles for $Fr = 0.40$ show distinct surface sharpening and evidence of localized wave breaking. In steady flows, surface curvature leads to the kinematic generation of vorticity equal to twice the local angular velocity multiplied by the local curvature (e.g. Lugt 1987; Rood 1995). Thus, where the surface is strongly distorted, i.e. highly curved, considerable surface vorticity results. Presumably, strong surface curvature and associated large velocity gradients will also assist this vorticity to first diffuse and then convect into the main flow to interact with existing wake vorticity.

As alluded to previously, the distinct sharpening of the surface shape that occurs for $Fr \gtrsim 0.35$ shown in the previous figure, is presumably due to the local Froude number in the gap, $Fr_L = \bar{u}/\sqrt{gh}$, approaching unity. Here, $\bar{u}$ is a measure of the velocity through the gap. For linear shallow-water waves, the Froude number is equal to the ratio of the flow speed to the wave speed. For waves to travel upstream requires $Fr_L < 1$. At higher Froude numbers, hydraulic jumps may form. These sudden changes in surface height correspond to changes from locally supercritical ($Fr_L < 1$) to locally subcritical ($Fr_L > 1$) flow (e.g. see Acheson 1990).

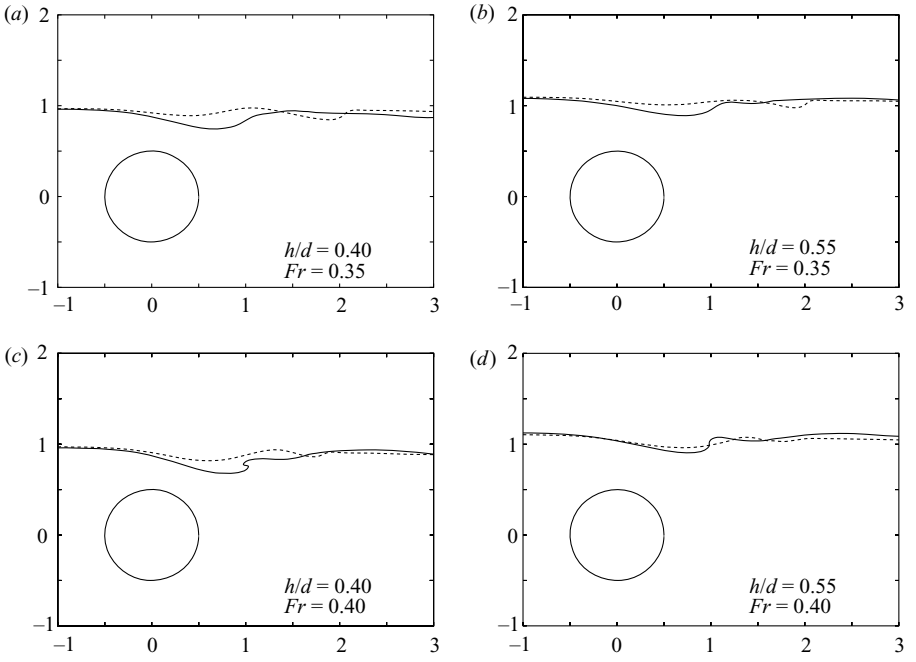

FIGURE 6. The surface position at the two extremes in the lift cycle for different Froude numbers and gap ratios (as marked). —, maximum lift; - - -, minimum lift.

To investigate whether the local Froude number was reaching critical values in the fluid above the cylinder, Fr_L was evaluated for a range of Froude numbers and gap ratios and the results are shown in figure 7. The maximum velocity through the gap at the time of maximum lift was used as the velocity scale for the local Froude number, but the curves are generally representative of the typical behaviour over a shedding cycle. For a gap ratio of $h/d = 0.4$, the local Froude number varies between $0.62 \leqslant Fr_L \leqslant 0.91$, corresponding to the global Froude number range $0.25 \leqslant Fr \leqslant 0.40$. Thus, not surprisingly, the local Froude number in the gap is considerably higher than the global Froude number for small gap ratios. Figure 6 shows that the surface distortion becomes very large, and possibly forms a breaking wave as Fr is increased from 0.35 to 0.40, for this gap ratio. The local Froude number for the $Fr = 0.40$ case approaches unity ($Fr_L = 0.91$) at the time of maximum lift. In fact, examination of figure 6(*c*) shows that as the fluid flows over the cylinder, the free-surface curvature is such that the distance between the cylinder and the surface is a minimum past the vertical centreline. Thus, the local Froude number based on h and the maximum velocity on the vertical centreline will be an underestimate of the maximum local Froude number. Hence, the local surface sharpening in this case is consistent with the local Froude number attaining or exceeding the critical value. Figure 7 also shows that Fr_L increases as the gap ratio is reduced, indicating that the critical global Froude number at which wave breaking occurs should decrease with gap ratio as might be expected.

3.4. *Strouhal number variation with gap ratio*

The behaviour of the Strouhal number with gap ratio is shown in figure 8. Again the Froude number is varied over the range $0.25 \leqslant Fr \leqslant 0.40$. The proximity of the surface causes an initial increase in the Strouhal number as the cylinder is moved towards

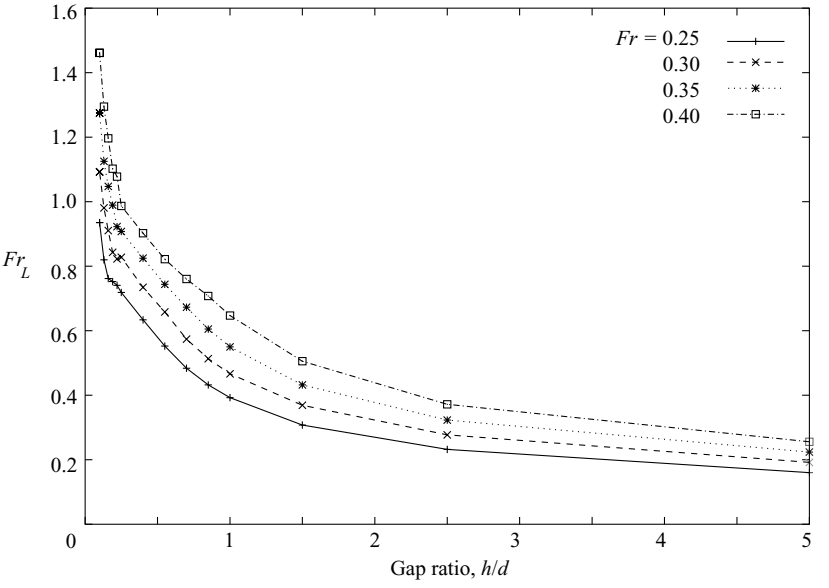

FIGURE 7. Variation of the local Froude number with gap ratio (the Froude number based on maximum velocity in the region directly above the cylinder), at both the points of maximum.

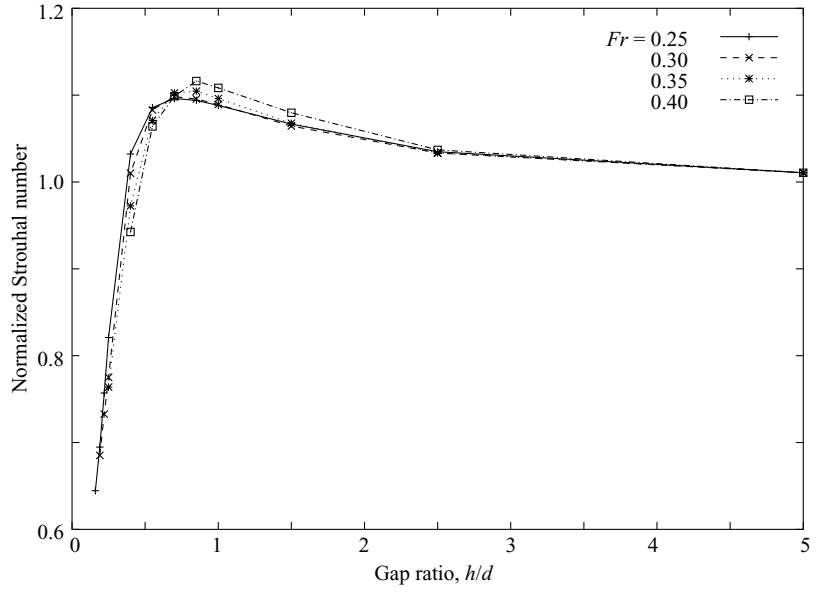

FIGURE 8. Variation of Strouhal number normalized with respect to Strouhal number of the reference cylinder, i.e. St/St_0) with gap ratio for Froude numbers of 0.25, 0.30, 0.35 and 0.40.

the surface, but this trend reverses as the gap ratio becomes small. The maximum Strouhal number occurs in the range $0.5 < h/d < 1.0$ and is a function of Froude number. The maximum increase is approximately 10 %.

While the trend in the Strouhal number is interesting in itself, the controlling mechanism is of greater interest. Green & Gerrard (1993) suggest that the period of vortex shedding is largely determined by the time taken for sufficient vorticity to

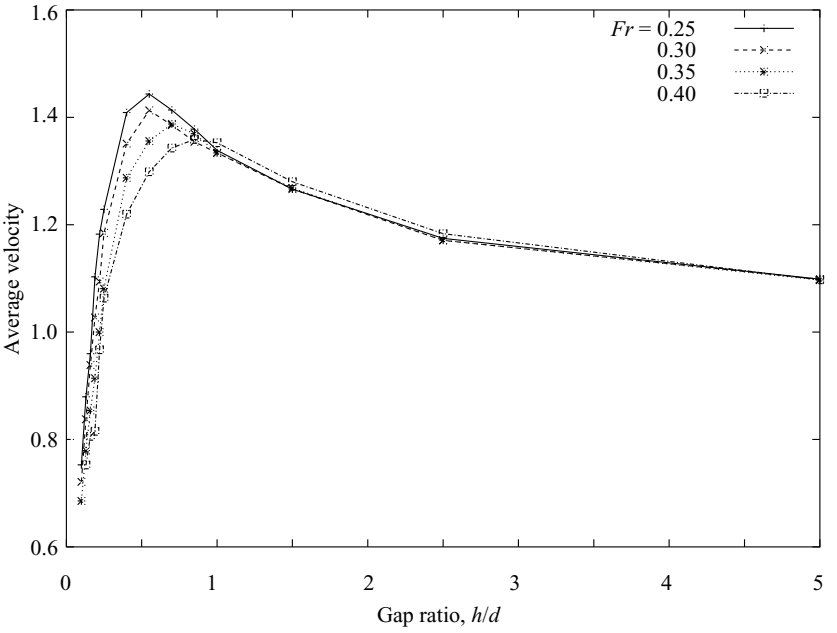

FIGURE 9. Plot showing the average velocity in the region directly above the cylinder as a function of gap ratio at the point of maximum lift, for Froude numbers of 0.25, 0.30, 0.35 and 0.40.

accumulate outside a region of high shear stress. Their model provides a possible explanation of the suppression of shedding observed by Strykowski & Sreenivasan (1990) when a small control cylinder is placed close to the large one. In addition, for the current problem, the supply of fluid into the vortex formation region is partially controlled by the presence of the free surface. It is hypothesized that the increase in period as the cylinder becomes close to the surface is due to the increase in the time required for fluid to collect in the vortex formation region, where it forms into discrete vortex structures. In turn, this time will be influenced directly by the proximity of the surface and the time-dependent nature of the surface. To investigate this hypothesis further, it is necessary to examine the transport of fluid through the gap between the cylinder and surface.

The height-averaged velocity through the gap at the time of maximum lift is given in figure 9. This figure illustrates the same trends as seen in the Strouhal number behaviour. As the Froude number is increased, the peak in the average velocity curve occurs at a higher gap ratio. As the gap becomes small, all the velocity curves approach the origin, as expected. The average velocity is closely related to the amount of circulation available to be shed into the wake. The curves indicate that as the gap is decreased, the transport of fluid into the wake decreases and the circulation is also reduced. This is consistent with the observed reduction in Strouhal number. Conversely, for intermediate gap ratios there is an increase in Strouhal number over the reference case. The average velocity curves are also consistent with this behaviour because of the increased flux of vorticity into the wake.

3.5. *Formation length*

Some changes to the observed wake behaviour may be associated with the position at which vortices form in the region behind the cylinder. This will certainly have an

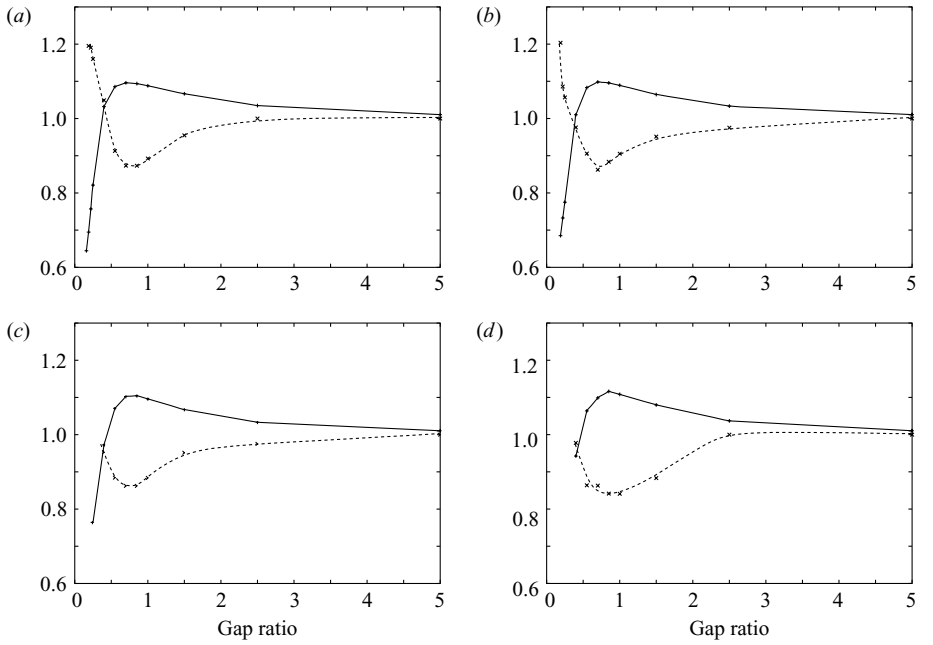

FIGURE 10. Variation of —, the normalized formation length (based on the standard deviation in the vorticity) and - - -, the normalized Strouhal number with gap ratio for Froude numbers (*a*) 0.25, (*b*) 0.30, (*c*) 0.35 and (*d*) 0.40.

impact on the magnitudes of the time-dependent forces. There does not appear to be a universally accepted definition of formation length in the literature, however, different methods tend to agree at least semi-quantitatively, and it is certainly a useful concept in understanding wake dynamics. Griffin (1995) reviews a number of ways of calculating the formation length. Two different ways of calculating the formation length were used for the current study. These measures are the distance from the cylinder to the point of maximum standard deviation of either vertical velocity or the vorticity. The methods give similar results.

Figure 10 reveals how the formation length (determined by the vorticity method) varies with gap ratio for Froude numbers in the critical range. Also shown is the variation in Strouhal number for each gap ratio. For each Froude number, the formation length decreases to a minimum as the gap ratio is reduced from a large value. The minimum occurs in the range $0.5 < h/d < 1.0$. As the gap ratio is further reduced, the formation length rapidly increases. The normalized Strouhal number curves are close to mirror images of the normalized formation length curves, indicating the strong association between these variables.

3.6. *Convective velocity of vortices*

The influence of the free surface on the path and speed of the shed vortices is of particular relevance to understanding the modification to the wake behaviour from the reference case. Figure 11 shows the region in the wake where the convection speeds of vortices were recorded. Note that for the smallest gap ratios and largest Froude numbers, the wake is not strictly periodic, however, the data presented provide a representative guide. The variation of the convective velocity with Froude number is shown in figure 12 for a discrete set of gap ratios. These results indicate that the

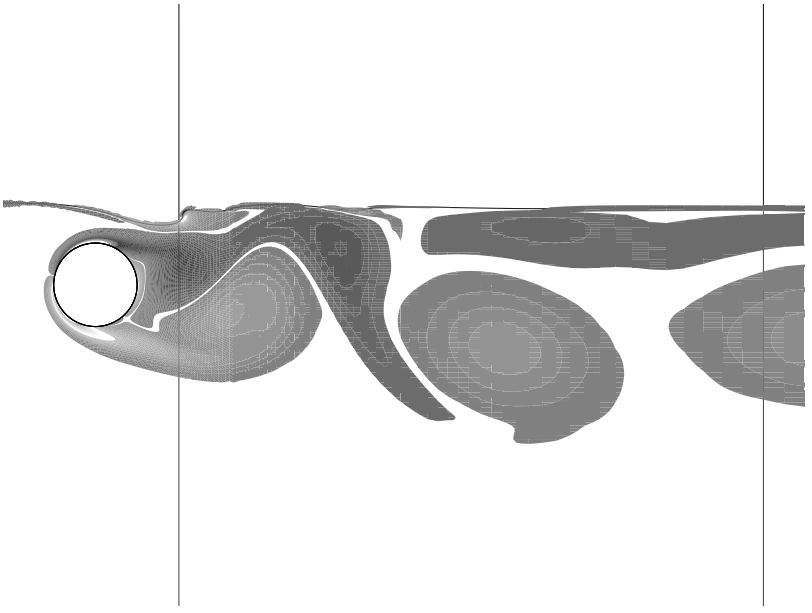

FIGURE 11. Plot showing the vorticity field for a gap ratio of 0.40 and a Froude number of 0.40. The Reynolds number for this case is 180. The two vertical lines denote the domain size used for calculating the vortex convection speeds and tracking the vortex paths.

convective velocity of the positive vortices originating from the bottom shear layer remains relatively constant or decreases only slightly with Froude number. However, the variation of convective vortex velocity with Froude number is a strong function of gap ratio. There is little effect for deep submergence. For small gaps, the convective velocity of the negative vortices is higher than the positive vortices, presumably owing to the image vortex on the other side of the surface aiding the forward motion. This situation reverses for large Froude numbers. In that case, the weakening of the negative vortices through entrainment and diffusion of, and cross-annihilation with, surface vorticity results in a significant change in wake dynamics. It is probably associated with the metastable states observed at even higher Froude numbers. The associated wake dynamics will be described in later sections.

3.7. *High-Froude-number cases and experimental comparisons*

Most experimental studies on the flow past submerged cylinders have been done at larger Froude numbers than were the focus of previous sections. High Froude numbers can result in large surface deformation with a corresponding significant impact on the wake development. Sheridan *et al.* (1995, 1997, 1998) and Hoyt & Sellin (2000) considered Froude-number and gap-ratio ranges that will be examined in this section.

The broadest range of parameter space was considered by Sheridan *et al.* (1997). They indicated that flow can be categorized loosely by the behaviour of the jet of fluid passing over the cylinder. Three basic wake states were identified where the jet (i) followed the free surface, (ii) occupied the space between the free surface and the cylinder, or (iii) remained attached to the cylinder so that it was almost directed vertically downwards. These wake states are not mutually exclusive, in that the flow may switch between them, either in a semi-regular way or through external interaction. In the comparisons that follow, numerical parameters were chosen to be as close as possible to the experimental values given the discrete coverage of the parameter space.

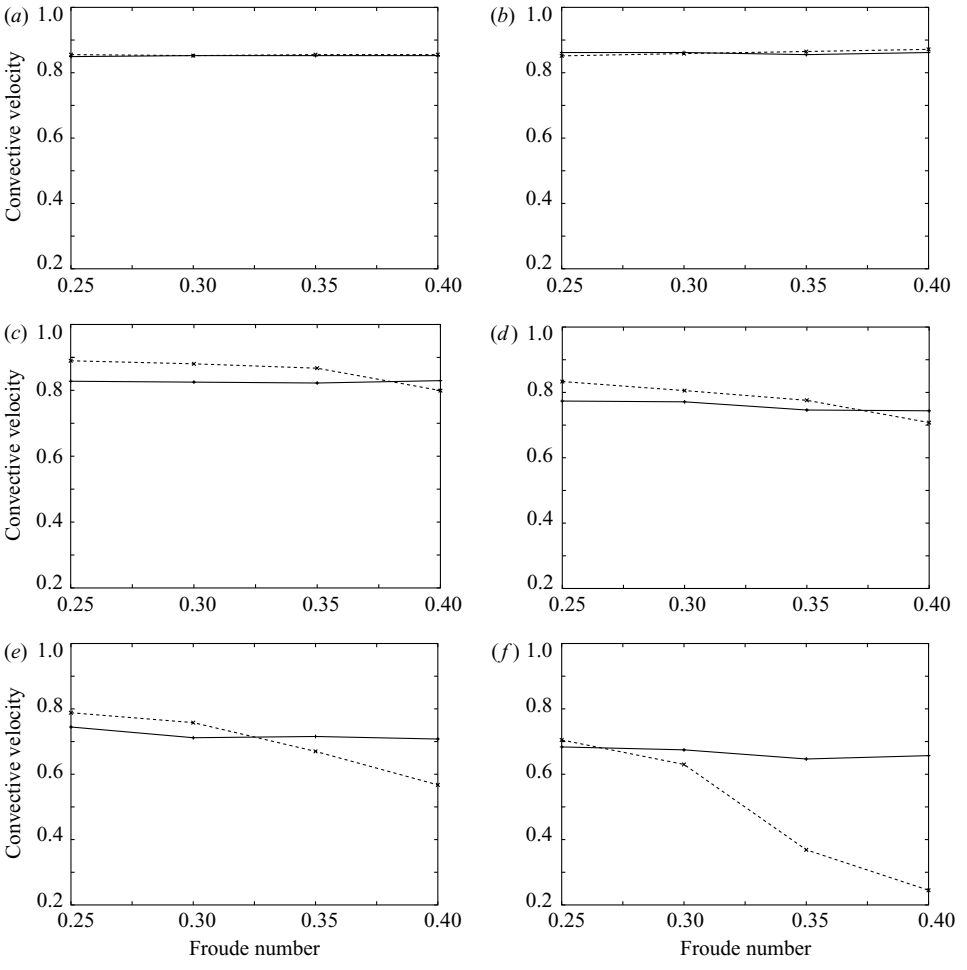

FIGURE 12. Plots showing the variation in vortex convection speed with Froude number for both the positive and negative vortices. (*a*) Gap ratio of 5.00, (*b*) 2.50, (*c*) 1.00, (*d*) 0.70, (*e*) 0.55 (*f*) 0.40 —, positive; - - -, negative.

Prior to presenting these numerical comparisons, it is worth summarizing the metastable states observed by Sheridan *et al.* (1995, 1997). Sheridan *et al.* (1997) note that at a Froude number of 0.60 for gap ratios in the range $0.75 \leqslant h/d \leqslant 0.24$, the jet tended to move progressively from a state of attachment to the free surface to being almost attached to the rear of the cylinder. Little information was provided on the time-dependent nature of the flow; however, it seems reasonable to assume that the wake was indeed time dependent. Hoyt & Sellin (2000) also examined this flow, but at a slightly lower Froude number of 0.53. Their dye visualizations clearly showed time dependence and distinct Strouhal shedding was noted for $h/d = 0.75$.

For some cases, Sheridan *et al.* (1995, 1997) found that more than one wake state could be observed at a fixed Fr–h/d combination. For these cases, the wake spontaneously changed from one state to another in a pseudo-periodic manner. The non-dimensional cycle time was not given, but it was noted that it was typically two orders of magnitude longer than the Strouhal period.

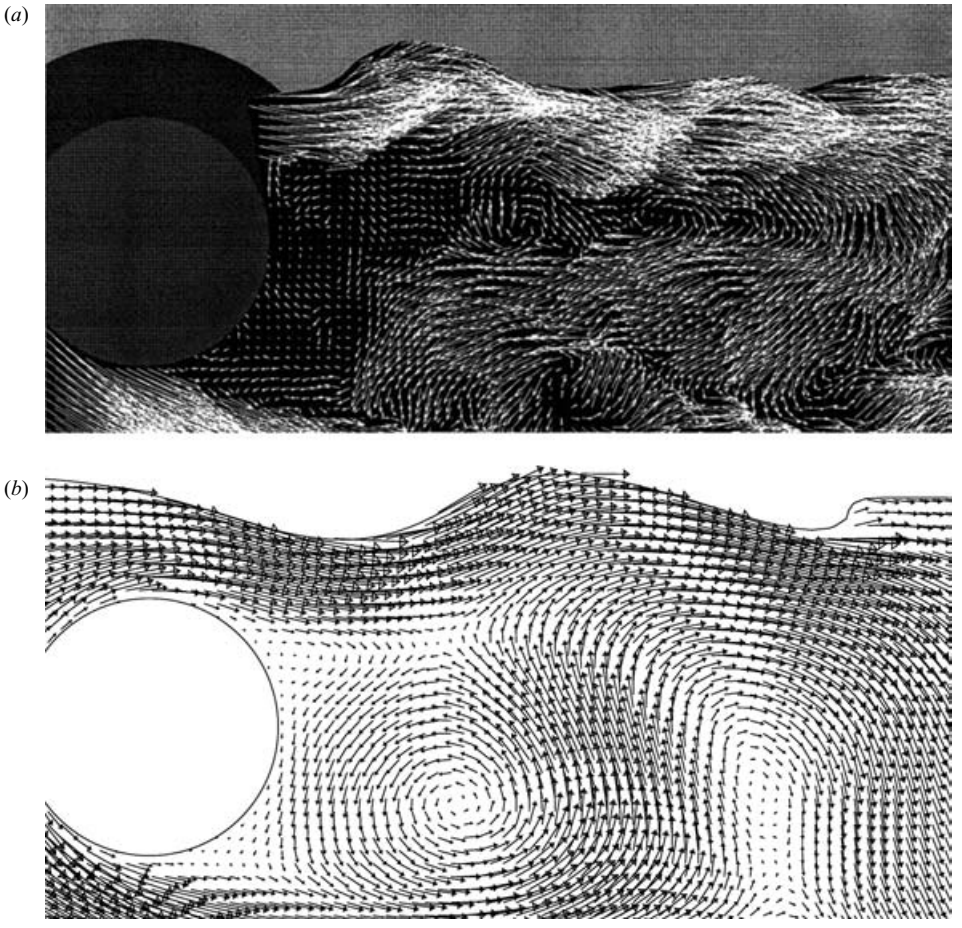

FIGURE 13. Comparison of the velociy fields between (*a*) the experimental results of Sheridan *et al.* (1997) (for $h/d = 0.40$, $Fr = 0.47$ and for a Reynolds number between 5990 and 9120, and (*b*) the numerically predicted results for $h/d = 0.40$, $Fr = 0.50$ and $Re = 180$.

The metastable behaviour observed by Sheridan *et al.* (1995) for parameters $Fr = 0.60$ and $h/d = 0.45$ involved the jet switching from a state of attachment to the surface to the intermediate position between the surface and the cylinder. They noted that the flow state could be switched to the other state by transiently piercing the free surface at a downstream position or temporarily altering the flow velocity. For the same Froude number and $h/d = 0.31$, the jet switched between the state of attachment to the rear of the cylinder and the intermediate state.

3.7.1. *Surface jets*

The first wake state described above, where the jet follows the surface, can be seen in figure 13. Numerically, the parameters are $Fr = 0.50$ and $h/d = 0.40$, which closely match the experimental values of $Fr = 0.47$ and $h/d = 0.40$. For the particular snapshots chosen, the comparison is remarkably good, despite the huge difference in Reynolds number. The amplitudes of the surface distortions are very similar, as is the surface jet width. The region of fluid in the near wake shows some differences, with the numerical velocity field much more coherent. Of course, this is not surprising

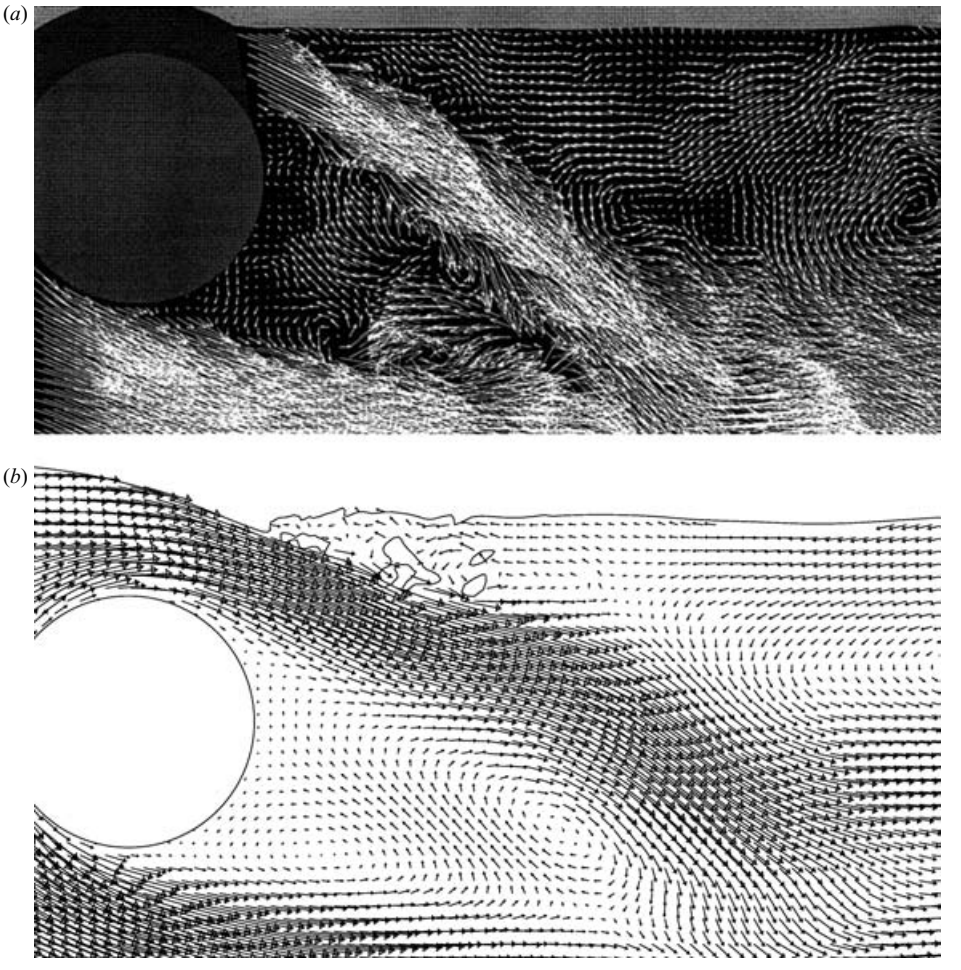

FIGURE 14. Comparison of the velocity fields between (*a*) the experimental results of Sheridan *et al.* (1997) for $h/d = 0.43$, $Fr = 0.60$ and for a Reynolds number between 5990 and 9120, and (*b*) the numerically predicted results at $h/d = 0.40$ (gap 5.9 diameters upstream is 0.45), $Fr = 0.60$ and $Re = 180$.

given the Reynolds number difference. In terms of vorticity (not shown), both the experimental and numerical results indicate there is only slight secondary surface vorticity entering the flow with subsequent entrainment by the surface jet.

In fact, the numerical simulations indicate that for this gap-ratio/Froude-number combination, the flow regularly switches between a state of attachment to the surface and the intermediate state in which it spends the majority of time. This flapping is at a much lower frequency than the shedding frequency, but the frequency is not well defined.

3.7.2. *Intermediate jets*

If the Froude number is increased slightly to $Fr = 0.60$, but with the same gap ratio, the tendency is for the jet to be deflected more. Figure 14 shows the comparison of wake velocity fields when the jet is directed into the intermediate region between the surface and cylinder. Again, the match is good. The deflection angles of the jet and the shear layer from the bottom of the cylinder are similar, as is the almost stagnant

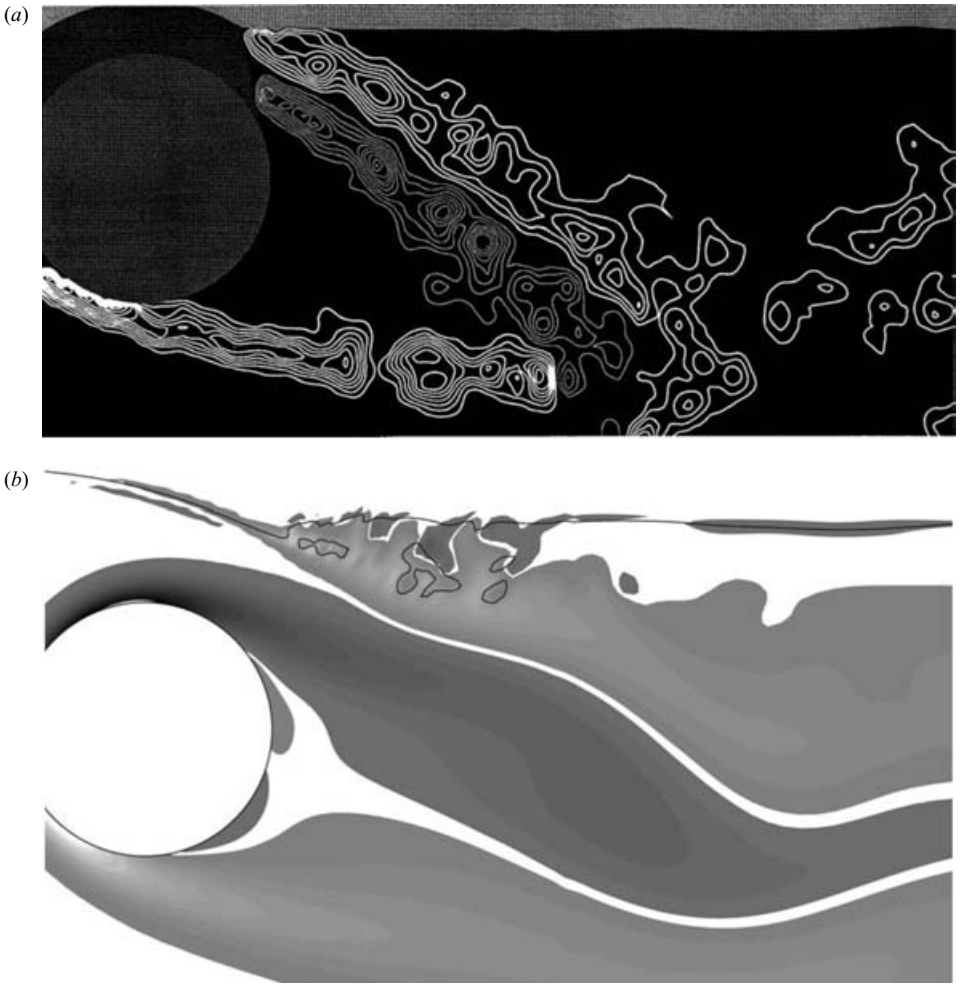

FIGURE 15. Comparison between (*a*) the experimental vorticity field of Sheridan *et al.* (1997) for $h/d = 0.43$, $Fr = 0.60$ and for a Reynolds number between 5990 and 9120, and (*b*) the numerically predicted vorticity field at $h/d = 0.40$ (gap 5.9 diameters upstream is 0.45), $Fr = 0.60$ and $Re = 180$.

region between the separating shear layers. The region of fluid above the jet is slowly recirculating upstream in both cases. There is also little surface distortion downstream apart from the adjustment in height as the fluid flows over the cylinder.

The bubbles appearing in the numerical simulation are due to minor entrainment of the light fluid into the heavy fluid as the jet penetrates (i.e. dives) into the relatively stagnant fluid at the rear of the cylinder. These also appear in some other simulations described later in this paper. Surface tension is not included in the numerical model, which will probably artificially enhance this process. Note that entrainment of bubbles is not mentioned in the experiments of Sheridan *et al.* (1997). In any case, the effect is relatively minor.

The experimentally derived and numerically simulated vorticity fields for this case are shown in figure 15. Of particular interest is the large amount of positive vorticity from the surface which enters the wake parallel to the main jet. The high vorticity flux has a significant effect on wake development, as described in more detail later. Vortex

shedding has effectively ceased at this time. The shear layers eventually reattach to the surface approximately 8 diameters upstream, encompassing a stagnation region with very little flow. At this point in the cycle, the character of the wake has changed such that the absolute instability is suppressed.

One notable difference between the experimental and numerical vorticity fields is the appearance of Kelvin–Helmholtz or Bloor–Gerrard vortices in the wake shear layers in the higher-Reynolds-number experimental flow. For the reference case these secondary vortices also develop strongly in this Reynolds-number range. Typically, they are associated with a shortening of the formation length; indeed, this is consistent with the slightly shorter formation length observed at the higher Reynolds number of the experiments.

3.7.3. *Jets attached to the cylinder*

The deflection of the jet increases if the gap ratio is reduced further to $h/d \simeq 0.30$. Recall that for these parameters, the experimental results of Sheridan *et al.* (1995, 1997) indicate that the jet switches from a state of attachment to the cylinder to the intermediate state. Figure 16 shows that experimental velocity field of Sheridan *et al.* (1997), the numerical velocity field and dye visualizations of Hoyt & Sellin (2000), all for approximately the same Froude number–gap ratio combinations. The angle of deflection of the jet is clearly greater than the previous case, and the stagnant region between the shear layers is smaller. Again, the region above the angled wake is slowly recirculating. No vortex shedding is observed for this combination of parameters. The wake state bears some resemblance to those calculated by Fornberg (1985) for flow past a cylinder with enforced symmetry about the centreline.

Figure 17 provides comparison of the vorticity fields. As for the previous combination of parameters, considerable positive vorticity enters the wake from the free surface. This vorticity results in the rapid and severe weakening of the top shear layer associated with the jet, through cross-diffusion and cross-annihilation.

3.7.4. *Very small gaps*

The final experimental comparison is for $Fr = 0.60$ and $h/d = 0.10$–0.16. Here, the gap is sufficiently small to lead to a significant reduction in the velocity and flux of fluid through the gap over previous cases. Coupled to this, the closeness of the surface results in increased diffusion into the surface and the strong convection of surface vorticity into the flow. These effects lead to only a weak rapidly dissipated jet, which is closely attached to the rear of the cylinder, as shown in figure 18. The region between the shear layers is now very small, and the recirculating flow above the jet has become almost stagnant. In fact, the recirculation region in the wake can be exceptionally long, typically reattaching more than 15 diameters downstream.

3.7.5. *Switching frequency*

It is difficult to determine accurate values of the switching frequency from numerical simulations because of the long time integration periods required and the irregularity of the signal. The $Fr = 0.55$ and $h/d = 0.40$ combination represents a case where the switching occurred relatively regularly for the simulations. A Fourier analysis of the lift signal indicated a strong modulation frequency of approximately 0.015. In contrast, the shedding frequency was about 0.21, about 14 times greater. Sheridan *et al.* (1997) indicated that for a similar case, the switching frequency was about two orders of magnitude smaller than the Strouhal frequency, although quantitative results were not given.

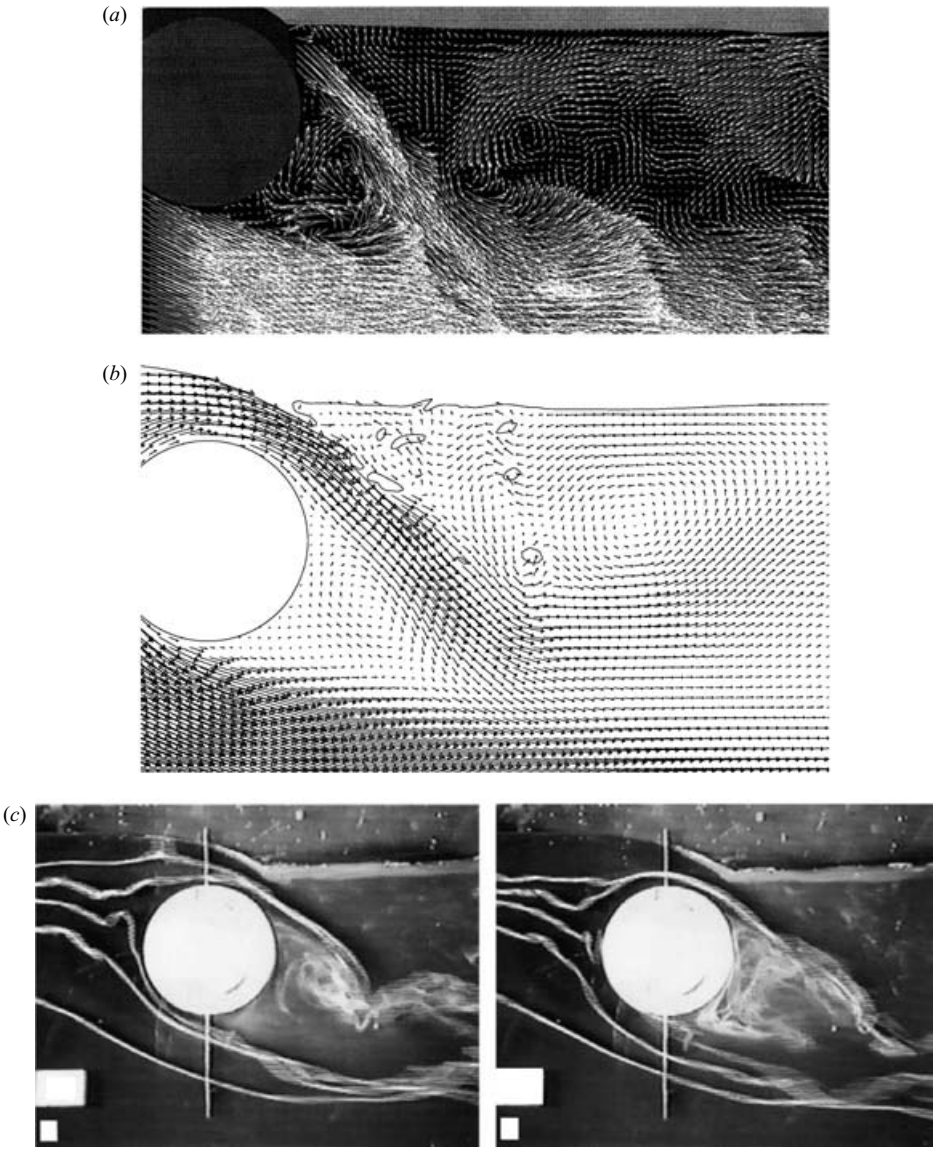

FIGURE 16. Comparison between (*a*) the experimental results of Sheridan *et al.* (1997) for $h/d = 0.31$, $Fr = 0.60$ and a Reynolds number between 5990 and 9120, (*b*) the current numerically predicted results at $h/d = 0.25$ (gap 5.9 diameters upstream is 0.26), $Fr = 0.60$ and $Re = 180$, and (*c*) experimental results of Hoyt & Sellin (2000) at $h/d = 0.31$, $Fr = 0.53$ and $Re = 27\,000$.

In any case, it might be expected that the switching frequency would be sensitive to Reynolds number and other factors. For example, inaccuracies in capturing wave breaking, the presence of turbulence and even the distribution of surfactants (e.g. Sarpkaya 1996) are likely to have a substantial effect on the switching frequency.

4. Discussion and conclusions

Results have been presented for the parameter space defined by $0.0 \leqslant Fr \leqslant 0.7$ and $0.1 \leqslant h/d \leqslant 5.0$. Generally, where comparisons can be made, the predictions

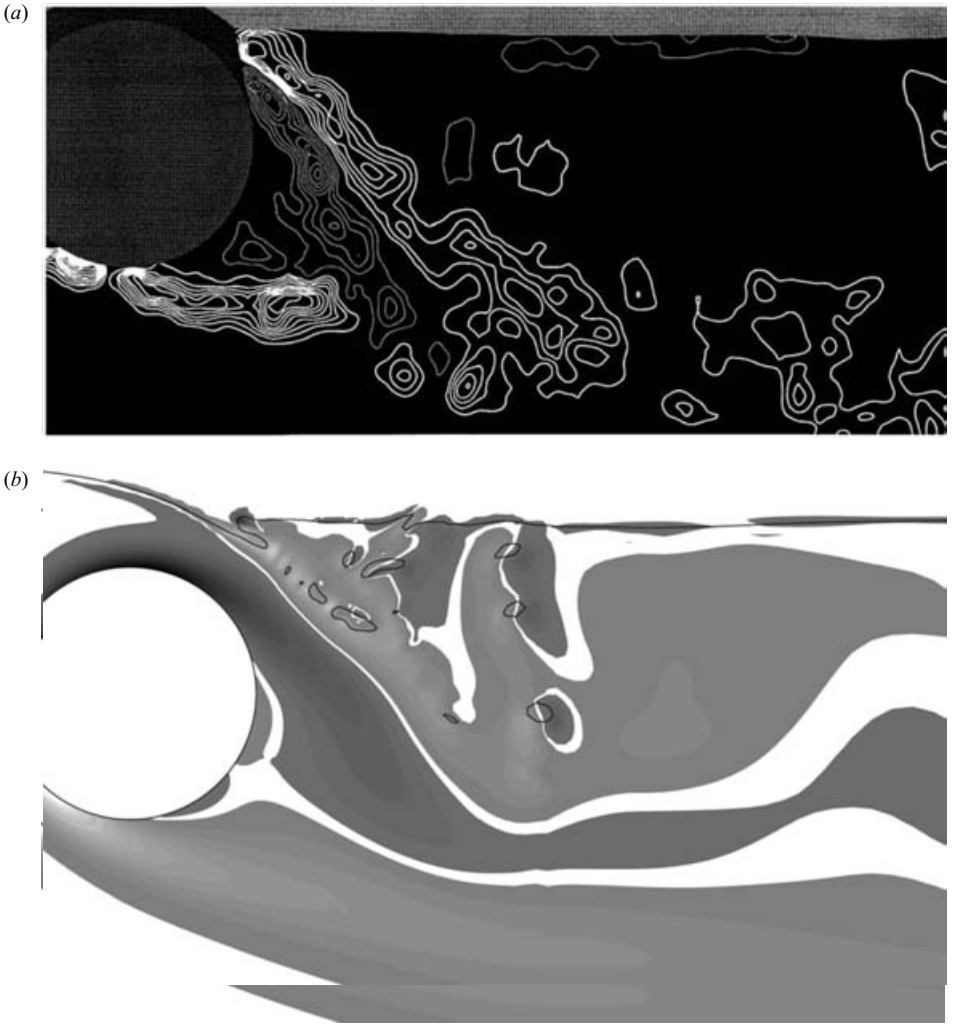

FIGURE 17. Comparison between (*a*) the experimental vorticity field of Sheridan *et al.* (1997) for $h/d = 0.31$, $Fr = 0.60$ and a Reynolds number between 5990 and 9120, and (*b*) current numerically predicted results at $h/d = 0.25$, $Fr = 0.60$ and $Re = 180$.

are in good agreement with previous results. The low-Froude-number results agree surprisingly well with previous predictions and experimentally observed behaviour for the flow past a cylinder near a no-slip boundary examined by a number of authors (e.g. Göktun 1975; Roshko *et al.* 1975; Bearman & Zdravkovich 1978; Angrilli *et al.* 1982; Price *et al.* 2000). In particular, the observed wake behaviour variation with gap ratio, and the Strouhal number, force coefficients and formation length show at least qualitative agreement.

Perhaps surprising is the relative sensitivity of surface deformation to Froude number. For example, for $h/d = 0.4$ and 0.55, figure 6 indicates that severe local surface deformation is minimal at $Fr = 0.35$, but substantial at $Fr = 0.40$. This appears to be due to the local Froude number in the gap reaching or exceeding the critical level of unity as the Froude number is incrementally increased. For smaller gap ratios, this transition occurs at slightly lower Froude numbers. Free-surface sharpening and

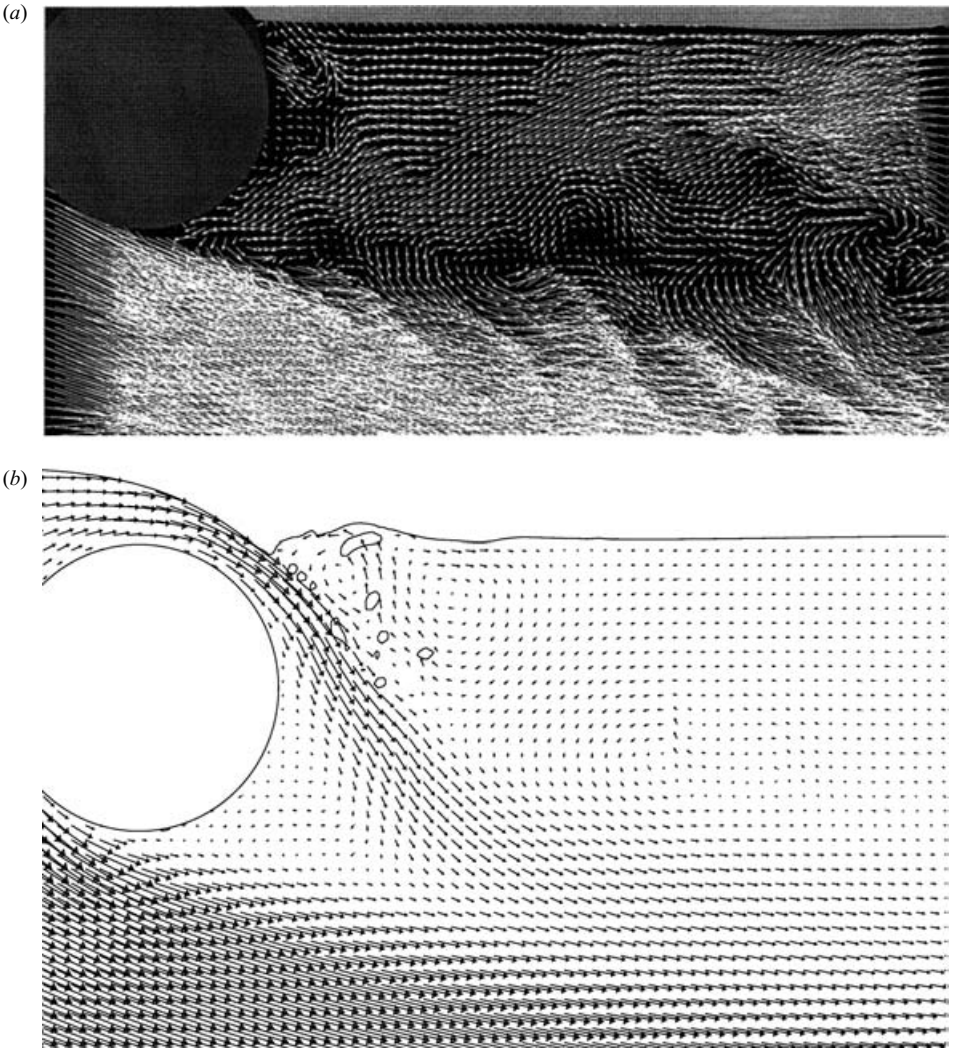

FIGURE 18. Comparison between (*a*) the experimental velocity field of Sheridan *et al.* (1997) at $h/d = 0.16$, $Fr = 0.60$ and a Reynolds number between 5990 and 9120, and (*b*) the numerically predicted velocity field at $h/d = 0.10$, $Fr = 0.60$ and $Re = 180$.

wave breaking can lead to the introduction of a substantial quantity of vorticity into the wake, which can interact with the top shear layer through diffusion and cross-annihilation, substantially changing the wake evolution. Apart from the greater amount of resident surface vorticity, high curvature allows easier entry of this surface vorticity into the wake. This is because diffusion away from the surface is more effective owing to the higher velocity gradients and it needs to act only over a short distance before convection can transport the vorticity away from the surface, since the velocity generally becomes non-parallel to the free surface over a short distance.

For small gaps, the convection velocity of the vortices formed from the top shear layer is strongly dependent on Froude number. At low Froude numbers, these vortices convect faster than their counterparts formed from the lower shear layer. This is due to the induced velocity from the image vortex on the other side of the surface.

However, as the Froude number is reduced, the convection velocity of these top vortices slow considerably.

Overall, the agreement with experimental studies, at Reynolds numbers typically 30–50 times larger, indicate that the flow is largely controlled by two-dimensional flow structures (vortex shedding, a diffusive flux of vorticity from curved surface and subsequent convection into the bulk flow). It appears that three-dimensionality and turbulence cause only relatively minor modifications to the wake evolution, as suggested by Sheridan *et al.* (1997).

The semi-periodic switching between wake states that can occur at high Froude numbers appears to be under the control of a feedback loop. The elements of this hypothesized feedback loop are described with reference to the parameter set $Fr = 0.55$ and $h/d = 0.40$, chosen because it shows clearly the intermediate wake states involved. This combination of parameters results in the top shear layer switching between attachment to the free surface and an intermediate state where it is angled between the cylinder and the free surface.

Figure 19 provides a sequence of images showing the evolution of the vorticity field as the jet flow switches between the attached and angled states, and back again. Each image corresponds to approximately the same phase in 10 consecutive Strouhal shedding cycles. Further examples of image sequences and animations showing this switching behaviour are given in Reichl (2001).

In terms of the feedback loop, consider an initial state where the jet is currently attached to the free surface (corresponding to the first image of figure 19).

(*a*) The formation of Strouhal vortices from the negative shear layer close to the surface induces strong time-dependent surface curvature, which in turn introduces substantial positive vorticity from the surface to cross-diffuse and cross-annihilate with the negative vorticity from the top shear layer. Over a few shedding cycles, this severely weakens the top shear layer. There is a strong asymmetry in the vorticity content of the upper and lower shear layers at the end of this phase.

(*b*) The top shear layer is now directed downwards and contains relatively less circulation per unit length than the bottom shear layer. Because of the near wake asymmetry, the absolute instability is at least partially suppressed, and Strouhal vortex formation and shedding become weaker over subsequent cycles. (Note that Koch (1985) has indicated that the absolute instability is destroyed by wake asymmetry).

(*c*) The weakening and redirection of the top shear layer, and the reduction in the formation of strong compact Strouhal vortices, lead to a reduction in the surface curvature and associated positive surface vorticity entering the flow. This allows the top shear layer to recover in strength and drift back towards the surface. As the shear-layer symmetry is re-established, the wake again becomes absolutely unstable and Strouhal shedding recommences.

Figure 9 shows that for small gap ratios, as the gap ratio is decreased, the average velocity of fluid moving through the gap rapidly decreases. Dimensional analysis indicates the flux of vorticity feeding into the shear layer depends on the square of the average velocity. Thus, the vorticity flux drops off very rapidly with decreasing gap ratio. For low Froude numbers, some diffusion into the surface, owing to the proximity of the shear layer to the surface, also acts to reduce the strength of the shear layer. For high Froude numbers, the effect is compounded by the introduction of positive vorticity at the surface, which enters the wake and further destroys the negative shear layer through cross-diffusion and cross-annihilation. Hence, it is not surprising that shedding ceases, leading to an extremely-long quasi-steady recirculation zone at the rear of the cylinder in this case.

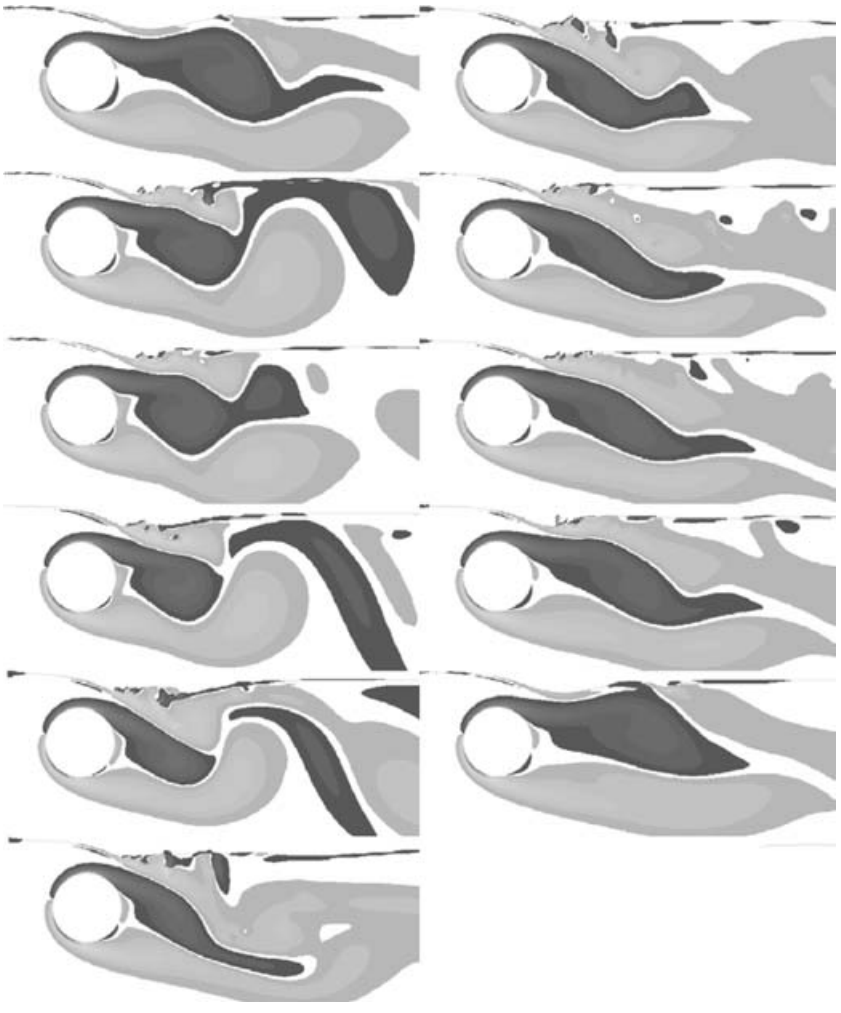

FIGURE 19. Evolution of the wake vorticity over a jet switching cycle for $Fr = 0.55$ and $h/d = 0.40$. Images correspond to approximately the same phase in consecutive Strouhal shedding cycles. The order of the sequence is column 1 followed by column 2.

For the metastable wake states it is not surprising that Sheridan *et al.* (1995) found that external disturbances to the downstream region could cause switching between states. Piercing the surface is likely to induce roll-up of the negative shear layer if the shear layer is already attached. This causes a chain of events resulting in the jet deflecting downwards. On the other hand, if the jet is already angled down, then piercing may disturb the large-scale recirculation which helps to sustain the deflected jet. If the recirculating flow is subsequently convected downstream, then the shear layer may reattach to the surface.

P. R. would like to acknowledge support provided through an Australian Post-graduate Award. The authors would like to acknowledge strong support from the Victorian Partnership for Advanced Computing and the Australian Partnership for Advanced Computing which enabled this research to take place.

REFERENCES

Acheson, D. J. 1990 *Elementary Fluid Dynamics*. Oxford University Press.

Angrilli, F., Bergamschi, S. & Cossalter, V. 1982 Investigation of wall induced modifications to vortex shedding from a circular cylinder. *Trans. ASME J. Fluids Engng* **104**, 518–522.

Barkley, D. & Henderson, R. D. 1996 Three-dimensional Floquet stability analysis of the wake of a circular cylinder. *J. Fluid Mech.* **322**, 215–241.

Bearman, P. W. & Zdravkovich, M. M. 1978 Flow around a circular cylinder near a plane boundary. *J. Fluid Mech.* **89**, 33–47.

Berger, E. & Wille, R. 1972 Periodic flow phenomena. *Annu. Rev. Fluid Mech.* **4**, 313.

Dimas, A. A. & Triantafyllou, G. S. 1994 Nonlinear interaction of shear flow with a free surface. *J. Fluid Mech.* **260**, 221–246.

Fornberg, B. 1985 Steady viscous flow past a circular cylinder up to Reynolds number 600. *J. Comput. Phys.* **61**, 297–320.

Göktun, S. 1975 The drag and lift characteristics of a cylinder placed near a plane surface. Master's thesis, Naval Postgraduate School, Monterey, California, USA.

Green, R. B. & Gerrard, J. H. 1993 Vorticity measurements in the near wake of a circular cylinder at low Reynolds number. *J. Fluid Mech.* **246**, 675–691.

Griffin, O. M. 1995 A note on bluff body vortex formation. *J. Fluid Mech.* **284**, 217–224.

Henderson, R. D. 1997 Nonlinear dynamics and pattern formation in turbulent wake transition. *J. Fluid Mech.* **352**, 65–112.

Hirt, C. W. & Nichols, B. D. 1981 Volume of fluid (vof) method for the dynamics of free boundaries. *J. Comput. Phys.* **39**, 201–225.

Hoyt, J. W. & Sellin, R. H. J. 2000 A comparison of the tracer and PIV results in visualizing water flow around a cylinder close to the free surface. *Exps. Fluids* **28**, 261–265.

Koch, W. 1985 Local instability characteristics and frequency determination of self-excited wake flows. *J. Sound Vib.* **99**, 53–83.

Lei, C., Cheng, L., Armfield, W. & Kavanagh, K. 1998 A numerical study of vortex shedding from a circular cylinder near a wall. In *Intl Conf. on Hydrodyn. Seoul, Korea*, pp. 699–704.

Lei, C., Cheng, L. & Kavanagh, K. 1999 Re-examination of the effect of a plane boundary on force and vortex shedding of a circular cylinder. *J. Wind Engng Indust. Aerodyn.* **80**, 263–286.

Leonard, B. P. 1979 A stable and accurate convective modelling procedure based on quadratic upstream interpolation. *Comput. Meth. Appl. Mech. Engng* **19**, 59–98.

Lugt, H. J. 1987 Local flow properties at a viscous free surface. *Phys. Fluids* **30**, 3647–3652.

Lugt, H. J. & Ohring, S. 1992 The oblique ascent of a viscous vortex pair toward a free surface. *J. Fluid Mech.* **236**, 461–476.

Lundgren, T. & Koumoutsakos, P. 1999 On the generation of vorticity at a free surface. *J. Fluid Mech.* **382**, 351–366.

Martin, J. C. & Moyce, W. J. 1952 Part iv. an experimental study of the collapse of liquid columns on a rigid horizontal plane. *Trans. Phil. Soc. Lond.* **244**, 312–334.

Miyata, H., Shikazono, N. & Kani, M. 1990 Forces on a circular cylinder advancing steadily beneath the free-surface. *Ocean Engng* **17**, 81–104.

Morkovin, M. K. 1964 Flow around circular cylinder as a kaleidescope of challenging fluid phenomena. In *ASME Symp. Fully Separated Flows*, pp. 102–118. Philadelphia, Pennsylvania, USA.

Ohring, S. & Lugt, H. J. 1991 Interaction of a viscous vortex pair with a free surface. *J. Fluid Mech.* **227**, 47–70.

Price, S. J., Smith, J. G., Leong, K., Paidoussis, M. P. & Sumner, D. 2000 Flow-visualization around a circular cylinder near to a plane wall. In *Flow Induced Vibration* (ed. Z. Staubli), pp. 105–112. Balkema, Rotterdam.

Reichl, P. J. 2001 Flow past a cylinder close to a free surface. PhD thesis, Department of Mechanical Engineering, Monash University (available at http://mec-mail.eng.monash.edu.au/p̃aul/personal/).

Reichl, P. J., Hourigan, K. & Thompson, M. C. 2003 The unsteady wake of a circular cylinder near a free surface. *Flow Turb. Combust.* **71**, 347–359.

Rood, E. P. 1995 Vorticity interactions with a free surface. In *Fluid Vortices* (ed. S. I. Green), chap. 16, pp. 687–730. Kluwer.

Roshko, A., Steinolfson, A. & Chattoorgoon, V. 1975 Flow forces on a cylinder near a wall or near another cylinder. In *Proc. 2nd US Conf. Wind Engineering Res., Fort Collins*. Paper IV-15, pp. 1–3.

Sarpkaya, T. 1996 Vorticity, free surface, and surfactants. *Annu. Rev. Fluid Mech.* **28**, 83–128.

Sheridan, J., Lin, J.-C. & Rockwell, D. 1995 Metastable states of a cylinder wake adjacent to a free surface. *Phys. Fluids* **7**, 2099–2101.

Sheridan, J., Lin, J.-C. & Rockwell, D. 1997 Flow past a cylinder close to a free surface. *J. Fluid Mech.* **330**, 1–30.

Sheridan, J., Lin, J.-C. & Rockwell, D. 1998 The interaction of a cylinder wake with a free surface. In *Proc. ASME Fluids Engng Div. Summer Meeting, FEDSM98-5689, Washington DC, USA*.

Strykowski, P. J. & Sreenivasan, K. R. 1990 On the formation and suppression of vortex 'shedding' at low Reynolds numbers. *J. Fluid Mech.* **218**, 71–107.

Taneda, S. 1965 Experimental investigation of vortex streets. *J. Phys. Soc. Japan* **20**, 1714–1721.

Taniguchi, S. & Miyakoshi, K. 1990 Fluctuating fluid forces acting on a circular cylinder and interference with a plane wall. *Exps Fluids* **9**, 197–204.

Triantafyllou, G. S. & Dimas, A. A. 1989 Interaction of two-dimensional separated flows with a free surface at low Froude numbers. *Phys. Fluids* A **1**, 1813–1821.

Tryggvason, G. 1988 Deformation of a free surface as a result of vortical flows. *Phys. Fluids* **31**, 955–957.

Tryggvason, G., Unverdi, S. O., Song, M. & Abdolahi-Alibeik, J. 1991 Interaction of vortices with a free surface and density interfaces. In *Lectures in Applied Mathematics, Vortex Dynamics and Vortex Methods* (ed. C. R. Anderson & C. Greengard), vol. 28, pp. 679–699. American Mathematical Society.

Versteeg, H. K. & Malalasekera, W. 1995 *An Introduction to Computational Fluid Dynamics: The Finite Volume Method*. Longman.

Wang, H. T. & Leighton, R. 1991 Direct calculation of the interaction between subsurface vortices and surface contaminants. In *Proc. 9th OMAE Conf. Houston, Texas, USA*, pp. 271–277.

Warburton, T. C. & Karniadakis, G. E. 1997 Spectral simulations of flow past a cylinder close to a free-surface. In *Proc. ASME Fluids Engng Div. Summer Meeting, FEDSM97-3389, Vancouver, British Columbia, Canada*.

Williamson, C. H. K. 1989 Oblique and parallel modes of vortex shedding in the wake of a circular cylinder at low Reynolds numbers. *J. Fluid Mech.* **206**, 579–627.

Williamson, C. H. K. 1996 Vortex dynamics in the cylinder wake. *Annu. Rev. Fluid Mech.* **28**, 477–539.

Yu, D. & Tryggvason, G. 1990 The free surface signature of unsteady two dimensional vortex flows. *J. Fluid Mech.* **218**, 547–572.